ARTICLE

Exploration of Chromophores for VCD Couplet in Biomolecularly Transparent Infrared Region

Received 00th January 20xx,
Accepted 00th January 20xx

DOI: 10.1039/x0xx00000x

Tohru Taniguchi,*[a] Mohamad Zarif Mohd Zubir, [b] Nobuyuki Harada[c] and Kenji Monde*[a]

Interactions of two chromophores such as carbonyl groups yield a strong VCD couplet that reflects molecular structures. Use of VCD couplets for biomacromolecular structural studies has been hampered by severe signal overlap caused by numerous functional groups that originally exist in biomacromolecules. Nitrile, isonitrile, alkyne, and azido groups show characteristic IR absorption in the 2300-2000 cm^{-1} region, where biomolecules do not strongly absorb. We herein examined the usefulness of these functional groups as chromophores to observe a strong VCD couplet that can be readily interpreted by theoretical calculations. Studies on a chiral binaphthyl scaffold possessing two identical chromophores showed that nitrile and isonitrile groups generate moderately-strong but complex VCD signals due to anharmonic contributions. The nature of their anharmonic VCD patterns is discussed by comparison with the VCD spectrum of a mono-chromophoric molecule and by anharmonic DFT calculations. On the other hand, through studies on a diazido binaphthyl and a diazido monosaccharide, we demonstrated that azido group is more promising for structural analysis of larger molecules due to its simple, strong VCD couplet whose spectral patterns are readily predicted by harmonic DFT calculations.

Introduction

Through-space interactions of two suitable chromophores yield an exciton circular dichroism couplet, i.e., a pair of positive and negative Cotton effects. The sign and intensity of the couplet reflects the absolute arrangement of the electric dipole transition moments (EDTMs) associated with the chromophores. This phenomenon has provided a basis for a structural analysis method using electronic circular dichroism (ECD) spectroscopy, named the exciton chirality method.[1-4] With proper understanding on EDTMs and the conformations of analyte molecules, the ECD exciton chirality method has revealed the structures of various small molecules[3, 5, 6] as well as medium-sized molecules (500 to 2,000 Da).[3, 7-9] Use of this method has often been associated with introduction of chromophores when the original molecules do not show informative or strong ECD signals. A repertoire of UV chromophores with various absorption coefficients and absorption wavelength such as *para*-substituted benzoyl groups have been applied.[2-4] Chromophores with a longer absorption wavelength (e.g., *para*-porphyrin-substituted benzoyl groups at 420 nm) are also available to extract structural information from molecules that are originally ECD-active to a spectrally transparent region, where the original molecules do not show informative signals.[10,11] Such chromophores have also been used to enhance ECD signals for submicromolar analysis.[3, 4] Careful use of chromophores with longer absorption maxima has enabled the analysis of much bigger molecules (e.g., biomacromolecules, polymers, and multimolecular systems).[12-15] However, such bulky, hydrophobic, π conjugated chromophores are less favourable for studying the native structures of biomacromolecules. Their bulkiness and complex electronic natures also significantly increase the computational cost when theoretical calculations are used to interpret exciton couplet.

Meanwhile, IR chromophores, which are much smaller and thus less perturb biomolecular structures, have been known to generate a vibrational circular dichroism (VCD) couplet. This phenomenon was originally studied under the name of coupled oscillator.[16] We reinvestigated VCD couplets stemming from C=O stretching vibrations of a series of small molecules and reported a correlation between the sign of the couplet and the dihedral angle θ of two carbonyl groups.[17, 18] On the basis of this correlation, structures of various molecules have been analysed with or without introduction of extra carbonyl chromophores, in a similar manner to the applications of the ECD exciton chirality method.[19-30] VCD couplet is also used for signal augmentation that leads to VCD measurements with reduced sample amount and with a short acquisition time. For example, VCD couplet of **1** was observed even at a concentration of 2.5 mM.[17] Such a VCD couplet approach obviously is not applicable to molecules with almost parallel or antiparallel carbonyl groups and should be used with care for flexible molecules and multichromophoric systems as is the case for the ECD exciton chirality method. Theoretical studies by other groups suggested that such VCD couplets are only partially due to excitonic

[a] *Frontier Research Center for Advanced Material and Life Science, Faculty of Advanced Life Science, Hokkaido University, Kita 21 Nishi 11, Sapporo 001-0021, Japan*
[b] *Graduate School of Life Science, Hokkaido University, Kita 21 Nishi 11, Sapporo 001-0021, Japan*
[c] *Institute of Multidisciplinary Research for Advanced Materials, Tohoku University, 2-1-1 Katahira, Aoba, Sendai 980-8577, Japan*
Electronic Supplementary Information (ESI) available: [details of any supplementary information available should be included here]. See DOI: 10.1039/x0xx00000x

interactions and warned about possible exceptions to this correlation.[31-34] Although such exceptions have not yet been experimentally witnessed for C=O vibrations, use of computations such as density functional theory (DFT) to interpret VCD couplets is highly recommended.

Structures and intermolecular interactions of biomacromolecules in the solution state have been studied using multiple analytical methods including ECD spectroscopy, fluorescence resonance energy transfer (FRET), and electron spin labels. The VCD couplet approach should serve as a new analysis tool with less physicochemical perturbation. Because biomacromolecules possess many carbonyl groups, extraction of their structural information needs introduction of IR chromophores with less overlap with their intrinsic IR absorption. ^{13}C isotope labelling has been used for this purpose to red-shift the C=O stretching frequency by ca. 40 cm^{-1}.[35] However, this shift is not sufficient to isolate the VCD signals without any overlap with ^{12}C=O and other vibrational signals. VCD couplets originating from other chromophores such as C=S, C-O, C=N and C-H have also been studied.[32, 33, 36-38] Yet to be examined are chromophores in the 2300-2000 cm^{-1} region, where the fundamental vibrational modes of common biomacromolecular functional groups do not exist.

Chromophores with X≡Y and X=Y=Z systems such as alkyne, nitrile, isonitrile, azido, allene, and carbodiimide exhibit characteristic IR absorptions in a spectrally transparent region for biomacromolecules. Some of these chromophores have been utilized as vibrational probes in biomacromolecular IR studies (e.g., oligonucleotide conformations, β-amyloid aggregation, and drug-protein interactions).[39-41] In the present work, we have studied the VCD spectra of **2**-**6** to test the applicability of -CN, -NC, -C≡CH, and -N_3 groups as a chromophore for observing their VCD couplet (Figure 1). Dicarbonyl **1** was also studied to show a typical VCD couplet. Allene and carbodiimide were excluded because of their axially chiral structures that yield strong intrinsic VCD signals on their own.[42-44] The core structure 2,2′-disubstituted-1,1′-binaphthalene was chosen as a C_2 symmetrical, rigid scaffold to regulate the distance (*r*) and the dihedral angle (θ) of the two chromophores. We aim for finding chromophores showing a strong VCD couplet whose shape is reliably predicted by theoretical calculations. An expected obstacle to this goal is that anharmonic vibrational contribution may be significant in the 2300-2000 cm^{-1} region and that its influence on the VCD spectra of chosen chromophores has not been studied. While this study focuses on small model molecules, the insight obtained here can be transferred to study larger molecules. Here, with using harmonic and anharmonic DFT calculations, we discuss the usefulness of these chromophores as well as their anharmonic behaviours.

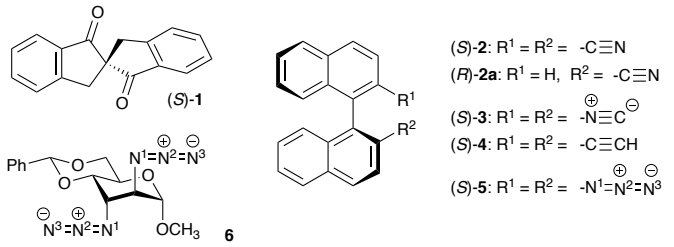

Fig. 1 Structures of **1**-**6**. Note that the stereochemical nomenclature becomes *R* for **2a**.

Experimental and computational details

Experimental details

Compounds **2**, **2a**, and **4** were prepared as a racemate starting from (±)-2,2′-dibromo-1,1′-binaphthyl and then enantioseparated using chiral column. Both enantiomers of **3** and **5** were synthesized from (*S*)- and (*R*)-1,1′-binaphthyl-2,2′-diamine. Compound **6** was synthesized from methyl α-D-glucopyranoside (see Supporting Information). For vibrational spectroscopy, each sample was dissolved in $CHCl_3$ or $CDCl_3$ and placed in a 50-μm or 100-μm BaF_2 cell. VCD and IR spectra were recorded using a JASCO FVS-6000 spectrometer with 4 cm^{-1} resolution for 1500 and 16 scans, respectively. Spectra in the 2300-2000 cm^{-1} region were measured using an InSb detector and an optical filter that passes through 2400-1900 cm^{-1} light, while those in the region below 1900 cm^{-1} were measured using an MCT detector with an optical filter that passes through light lower than 2200 cm^{-1}. The modulation frequency of the photoelastic modulator was set to 2127 cm^{-1} (for the measurement of 2300-2000 cm^{-1}) or 1350 cm^{-1} (for the measurement below 1900 cm^{-1}). With these spectrometer settings, each sample showed a virtually mirror-image VCD spectrum to its enantiomer in the 2300-2000 cm^{-1} region (Figure S1). To obtain more accurate spectra, the VCD spectra of *S* enantiomers of **1**-**5** were corrected by their *R* enantiomers using the following equation.

$$\Delta\varepsilon(S)_{corrected} = 1/2[\Delta\varepsilon(S)_{raw} - \Delta\varepsilon(R)_{raw}]$$

The VCD spectrum of **6** and all the IR spectra were corrected by solvent spectra obtained under the identical measurement conditions.

Computational details

DFT calculations were carried out on Gaussian 16 package.[45] Initial conformational search was carried out using molecular mechanics on Spartan 18 program.[46] Obtained geometries within 20 kJ/mol from the most stable were submitted to DFT optimization at B3PW91/6-311++G(d,p) level of theory, which predicted only one conformer for each compound within 2.0 kcal/mol energy window. For these geometries, IR and VCD spectra were calculated using the same level of theory. The calculated frequencies, dipole strength, and rotational strength were converted to IR and VCD spectra on GaussView 6 software using a peak half-width at half height of 6 cm^{-1}. Anharmonic calculations of **2**, **2a**, and **3** were performed on a default program implemented in Gaussian 16. Calculated frequencies were scaled using factors mentioned in figure captions.

Results and discussion

Conformational analysis and harmonic vibrational calculations

To study the relative orientation of the two chromophores in **1**-**5**, MMFF conformational search and the following structural optimization at DFT/B3PW91/6-311G++(d,p) were carried out for their (*S*)-enantiomers. Only one stable conformer each existed for **2**-**4** due to the rigidity of the binaphthalene scaffold and the *sp* hybridized linear shape of nitrile, isonitrile, and alkyne (Figure 2a). For the calculations of **2**, chloroform molecules coordinating to nitrile groups are explicitly included as this treatment provided a better VCD agreement in the case of anharmonic calculations (vide infra). Dicarbonyl model compound **1** also displayed only one conformer. Interestingly, compound **5** also showed only one conformer within a 2.0 kcal/mol energy window despite the rotatable σ bonds between the naphthalene moiety and the chromophoric substituents. See Figure S2a for computational results of less stable conformers of **5**.

Using these conformers, *r* and θ of **1**-**5** were analysed. This work defined these values based on the ideal localization of the vibrational motions of these chromophores. Namely, *r* was defined as the distance between two centres of the masses of atoms consisting of C=O bond (for **1**), each triple bond (for **2**-**4**), or of azido (for **5**), whereas θ was defined as the dihedral angle made by four atoms consisting of two C=O bonds (for **1**) or triple bonds (for **2**-**4**), or by the four terminal nitrogen atoms N3, N1, N1′, and N3′ (for **5**). Except for **1** and **5**, two chromophores in these structures were oriented with *r* and θ values of ca. 4 Å and +90°, respectively (Figure 2a and Table 1).

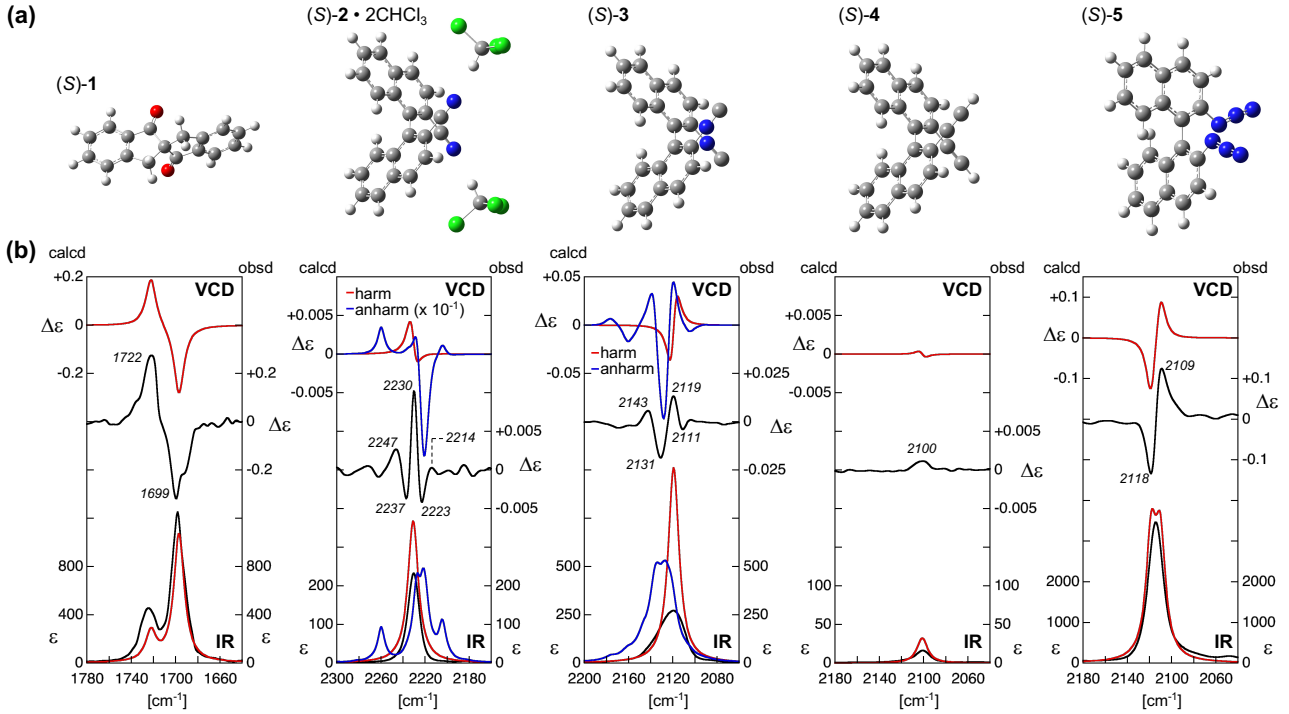

Fig. 2 (a) Most stable conformers of (*S*)-**1**, (*S*)-**2**•2CHCl$_3$, (*S*)-**3**, (*S*)-**4**, and (*S*)-**5**. (b) VCD (top) and IR (bottom) of measured (black) and calculated (red for harmonic DFT and blue for anharmonic DFT) spectra. Wavenumbers at the extrema of observed VCD signals are labelled in italic. Measurement conditions: *c* 0.04 M in CDCl$_3$ (for **1**), 0.2 M in CHCl$_3$ (for **2** and **3**), 0.6 M in CHCl$_3$ (for **4**), or 0.04 M in CHCl$_3$ (for **5**); *l* 50 μm. Calculation conditions: B3PW91/6-311++G(d,p). Frequency scaling factors: 0.953 (for **1**), 0.951 (for **2**, harmonic), 0.967 (for **2**, anharmonic), 0.966 (for **3**, harmonic), 0.987 (for **3**, anharmonic), 0.952 (for **4**), and 0.930 (for **5**).

Table 1 Interchromophoric distance (r) and dihedral angle of two chromophores (θ) of the most stable conformers of **1**-**6**, and predicted scaled frequencies (ν_n), dipole strengths (D_n), and rotational strengths (R_n) for the stretching vibrations of the discussed chromophores calculated at harmonic DFT/B3PW91/6-311++G(d,p). See captions of Figure 2-4 for the applied scaling factors.

	(*S*)-**1**	(*S*)-**2** • 2$CHCl_3$	(*S*)-**3**	(*S*)-**4**	(*S*)-**5**	(*R*)-**2a** • $CHCl_3$	**6**
r [Å]	3.2	4.3	4.2	4.4	5.3	–	5.6
θ [°]	-116	+97	+95	+94	-23	–	+122
ν_1 [cm^{-1}]	1696.9	2230.7	2118.7	2101.1	2110.2	2227.6	2107.1
D_1 [10^{-40} esu^2 cm^2]	1034	120	424	11.7	2124	160	1846
R_1 [10^{-44} esu^2 cm^2]	-706	-239	+537	+23.6	+260	+2.3	+378
ν_2 [cm^{-1}]	1722.2	2230.9	2119.8	2101.3	2118.4	–	2118.9
D_2 [10^{-40} esu^2 cm^2]	232	152	381	13.7	2169	–	558
R_2 [10^{-44} esu^2 cm^2]	+483	+243	-545	-25.0	-316	–	-558

Fundamental vibrational transitions of the most stable conformers of **1**-**5** were calculated using harmonic DFT calculations at the B3PW91/6-311++G(d,p) level of theory. Two fundamental vibrational modes were predicted in the 2300-2000 cm^{-1} region for each **2**-**5**. Corresponding C=O stretching modes of **1** were predicted at around 1700 cm^{-1} (scaled frequency). The dipole strength D_n and the rotational strength R_n associated with these vibrational modes are summarized in Table 1 and the simulated VCD and IR spectra based on these values are shown in Figure 2b. Among **1**-**5**, D_n and R_n values of dialkyne **4** were 10 to 100 times smaller compared to those of the other molecules, as expected from the non-polar nature of -C≡CH group, which leads to very weak IR absorption for C≡C stretching. This indicated experimental difficulties in observing a VCD couplet of **4**. R_n of **1**, **2**, **3**, and **5** were predicted to be in the same order of magnitude despite the differences in the values of r, θ, and D_n. Nevertheless, due to the small frequency differences of the two harmonic modes ($\nu_2 - \nu_1$) of **2** and **3**, their positive and negative components were predicted to mostly compensate each other. The frequency of the two azido vibrational modes of **5** differ by 8 cm^{-1}, which gave rise to a predicted strong VCD couplet.

Experimental spectra of dinitrile, diisonitrile, and dialkyne compounds

VCD spectra in the 2300-2000 cm^{-1} region have rarely been documented, especially since the development of Fourier-transform (FT) VCD spectrometers.[44, 47-50] To achieve a high S/N ratio in this region, we inserted an optical filter that passes through 2400-1900 cm^{-1} light to a FT-VCD spectrometer and used an InSb detector. Furthermore, to maximize the reliability of the observed spectra, both enantiomers of **2**-**5** were prepared and the VCD spectra of the enantiomeric pairs were compared. Each enantiomeric pair showed almost mirror-image VCD patterns in the 2300-2000 cm^{-1} region (Figure S1), which validated the accuracy of the VCD measurement in this region. The following spectral analysis is based on the "enantiomer-corrected" VCD spectra of (*S*)-enantiomers of **1**-**5** (Figure 2b).

Two nitrile groups (**2**) and isonitrile groups (**3**) gave rise to VCD signals with $\Delta\varepsilon$ of an order of 0.01, while two azido groups (**5**) and carbonyl groups (**1**) generated 10- to 100-fold stronger VCD absorption. Meanwhile, **4** showed a negligibly small VCD band with very small IR absorption ($\Delta\varepsilon$ 0.001 and ε 16 at 2100 cm^{-1}), consistent with the calculated small D_n and R_n values. Thus, we concluded that the terminal C≡CH group is not suitable for sensitively observing VCD couplet.

A VCD couplet originating from C=O stretching vibrations is presented by (*S*)-**1** ($\Delta\varepsilon$ -0.31 at 1699 cm^{-1} and $\Delta\varepsilon$ +0.27 at 1722 cm^{-1}). In this case the IR absorption bands also split. Its negative-positive VCD couplet was well reproduced by harmonic DFT calculations (Figure 2b). In contrast, the observed VCD of dinitrile **2** and diisonitrile **3** were more complex and showed a greater number of peaks compared to the harmonically calculated simple VCD spectra. With alternating positive and negative patterns of the observed VCD spectra, reliable interpretation of these VCD spectra in terms of VCD couplet is not possible. Similarly, attempts to correspond the harmonically predicted VCD signals of **2** and **3** to two of the observed VCD peaks are not appropriate. Previous VCD studies on deuterated molecules reported somewhat similar VCD patterns in the 2300-2000 cm^{-1} region and ascribed these to anharmonic VCD signals.[48, 49] Indeed, the IR band of **3** at 2119 cm^{-1} showed a wider skirt on the higher frequency side, which indicated involvement of anharmonic signals. Dinitrile **2** yielded a more symmetrical IR band, but nitrile groups are also known to exhibit anharmonic signatures in biomolecular IR studies.[51] Therefore, the complex, yet strong VCD features of **2** and **3** were ascribed to anharmonic VCD signals involving -CN and -NC vibrations, respectively.

Analysis of anharmonic VCD features of dinitrile and diisonitrile compounds

As mentioned earlier, this work aims for identifying chromophores exhibiting a strong VCD couplet that can be interpreted by theoretical calculations toward its applications to structural analysis of biomacromolecules. Nitrile and Isonitrile groups showed strong VCD signals, but the complex signal patterns seemed disadvantageous for structural analysis. Nonetheless, the usefulness of nitrile functionality as an IR reporter in biochemistry and the scarcity of insight into anharmonic VCD in the 2300-2000 cm^{-1} region prompted us to further investigate the VCD of **2** and **3** regarding on the following two questions:

(1) Harmonic VCD signals are known to be augmented by interactions of two IR chromophores, but are anharmonic VCD signals also augmented by such interactions?

(2) Are these anharmonic VCD spectra still useful for extracting structural information of the analyte molecule by using anharmonic DFT calculations?

To address the first question, mononitrile (*R*)-**2a** was synthesized to analyse its VCD spectrum in comparison with that of dinitrile (*S*)-**2**. Mononitrile **2a** was prepared as a racemate and then enantioseparated using CHIRALPAK® IB column, which led to the first-eluted (*S*)-(−)-**2a** and the second-eluted (*R*)-(+)-**2a** (Figure 3a, Figure S3).[52] Enantiopure (*R*)-**2a** showed an IR band at 2228 cm^{-1} whose intensity is half of that found for dinitrile (*S*)-**2** (Figure 3b). Meanwhile, no discernible VCD signals were observed for (*R*)-**2a**. Both harmonic and anharmonic (vide infra) DFT calculations of (*R*)-**2a**•$CHCl_3$ (Figure 3c) predicted ca. 100-fold smaller VCD signals compared to those calculated for **2** (Table 1 and Figure 3b). These results, for the first time, experimentally verified that interactions of chromophores enhance anharmonic VCD intensity.

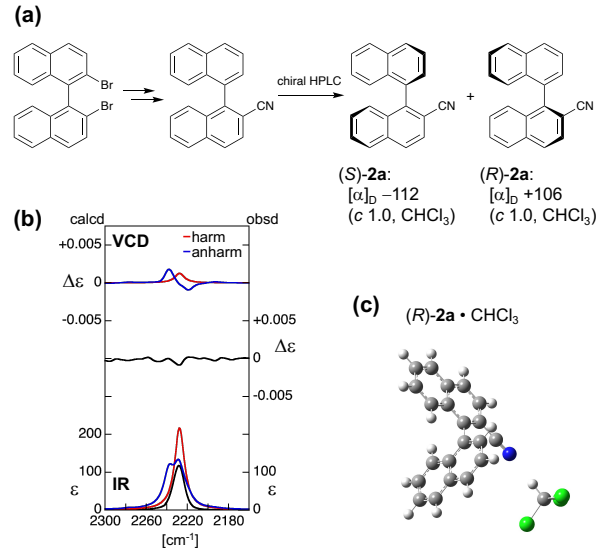

Fig. 3 (a) Preparation of enantiomerically pure **2a**. (b) VCD (top) and IR (bottom) of measured (black) and calculated (red for harmonic DFT and blue for anharmonic DFT) spectra of (*R*)-**2a**. (c) Most stable conformer of (*R*)-**2a**·$CHCl_3$. Measurement conditions: *c* 0.2 M in $CHCl_3$, *l* 100 μm, VCD spectrum of (*R*)-(+)-**2a** was corrected by that of (*S*)-(−)-**2a**. Calculation conditions: B3PW91/6-311++G(d,p). Frequency scaling factors: 0.950 (for harmonic) and 0.967 (for anharmonic).

Regarding on the second question, because the complex VCD signals of **2** and **3** were generated by interplays of two chromophores, the spectral patterns should reflect the orientation of chromophores as well as their local environment. Interpretation of anharmonic VCD spectra by means of anharmonic calculations has been reported,[53, 54] but their utility in the 2300-2000 cm^{-1} region has not been studied. Aiming at correlating anharmonic VCD signals with molecular structures, we performed VCD calculations of (*S*)-**2** and (*S*)-**3** using anharmonic DFT settings implemented in Gaussian 16 program. Among several functionals and basis sets tested, B3PW91/6-311++G(d,p) level well reproduced the observed VCD features of **3** (Figure 2b). Namely, experimentally observed small negative band at 2111 cm^{-1}, strong positive band at 2119 cm^{-1}, strong negative band at 2131 cm^{-1}, and moderately strong positive band at 2143 cm^{-1} were all seen in the calculated spectrum with similar shape and intensity. Application of the same level of theory to (*S*)-**2** with two explicit chloroform molecules resulted in a VCD spectrum partially similar to the observed one. The observed positive VCD peak at 2230 cm^{-1} and negative one at 2237 cm^{-1} may have cancelled out in the anharmonically predicted VCD spectrum. Comparison of the observed spectra and anharmonically calculated ones in the region below 1900 cm^{-1} also showed a moderate agreement (Figure S4). Overall, these preliminary results showed promise for deducing molecular structures from anharmonic VCD signals.

These results also highlighted obstacles to be overcome for studying biomacromolecules using these chromophores. First, the high computational cost for anharmonic DFT (ca. 100 times longer computational time than harmonic DFT) hampers the VCD calculations of many candidate structures. Second, solvent effects may be properly included into VCD calculations to well reproduce observed spectral patterns.[55] In the case of dinitrile **2**, solvent effects (e.g., implicit and explicit) drastically changed predicted anharmonic VCD results (Figure S5). Last, the dependence of the predicted VCD shape to the basis set and functional of a given system is yet to be investigated. See Figure S5 for anharmonic VCD spectra of **2** predicted by other calculation conditions. Although investigation of the second and last points are in progress by our group, chromophores with less anharmonic nature seem more practical.

VCD couplet by diazido compounds

Unlike nitrile and isonitrile chromophores, the interaction between two azido groups in (*S*)-**5** produced a rather simple positive-negative VCD couplet. This observation was in line with the previous insight that accidental Fermi resonance is less obvious for azido group.[40, 56] Moreover, the observed VCD intensities (Δε +0.12 at 2109 cm^{-1} and Δε -0.13 at 2118 cm^{-1}) are one order higher than those of nitrile and isonitrile (Figure 2b). This positive-negative couplet was accurately reproduced by harmonic VCD calculations of (*S*)-**5**. Thus, azido group fulfills the aforementioned requirements as VCD chromophores to extract structural information of biomacromolecules.

To test the applicability of azido group to biomolecules, we prepared a diazido monosaccharide derivative **6**, whose azido

groups are connected to sp^3 aliphatic carbons. The experimental VCD spectrum of **6** in $CHCl_3$ showed a strong positive-negative couplet without any obvious anharmonic VCD signals ($\Delta\varepsilon$ +0.10 at 2104 cm^{-1} and $\Delta\varepsilon$ -0.034 at 2119 cm^{-1}) (Figure 4a). Such a positive-negative couplet of **6** was also observed in a DMSO-h_6 – H_2O (9:1) mixed solvent (Figure S6). We also carried out MMFF conformational search and the following DFT structural optimization to investigate the orientation of the azido groups in **6**. Despite the rotatable nature of the σ bonds between the azido group and the pyranose ring, only one conformer with *r* of 5.6 Å and θ of +122° was found within a 3.0 kcal/mol energy window at B3PW91/6-311++G(d,p) (Figure 4b). The second most stable conformer with ΔE = 3.12 kcal/mol differed only in the rotation of C1 methoxy group (Figure S2b). Harmonic VCD calculations of the most stable conformer well reproduced the positive-negative couplet (Figure 4a), which supported the applicability of azido chromophores to structural analysis of biomolecules. Spectral agreement between the observed and the calculated was also seen in the region below 1600 cm^{-1} (Figure S7). Azido VCD couplets are reliably predicted also with using a smaller level of theory (B3PW91/6-31G(d)) as shown in Figure S8. Another practical advantage of azido is that protocols for its incorporation to various biomolecules have been established and some of azido-containing biomolecules (e.g. amino acids and sugars) are commercially available owing to the development of bioorthogonal alkyne-azide chemistry.[57] Application of azido groups to more complex molecular systems should be reported in due course.

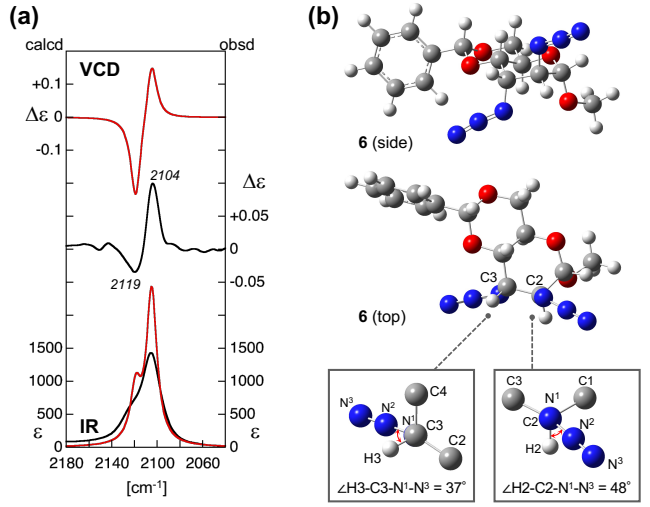

Fig. 4 (a) VCD (top) and IR (bottom) of measured (black) and calculated (red) spectra of **6**. (b) The most stable conformer of **6**. Newman projections for C2-N and C3-N bonds are shown at the bottom, in which dihedral angles made by azido group and methine C-H are illustrated by red arrows. Measurement conditions: *c* 0.04 M in $CHCl_3$, *l* 50 μm. Calculation conditions: harmonic DFT at B3PW91/6-311++G(d,p). Frequency scaling factor: 0.927.

Clockwise orientation of two azido groups of **6** showed a positive-negative VCD couplet, while anticlockwise **5** with a small dihedral angle (θ –23°) also exhibited a positive-negative couplet. Thus, azido VCD couplets of **5** does not follow a coupled oscillator model.[16] The stretching vibrations of two azido groups in both **5** and **6** were predicted to be out-of-phase for the lower frequency transition and in-phase for the higher frequency one. To obtain further insight into the relationship between the chromophoric orientation and the signal pattern, we calculated the VCD spectra of two azidomethane (CH_3-N_3) molecules and two azidobenzene (Ph-N_3) molecules. VCD computations of these model systems with 10° incremental changes of θ showed a clear dependence of VCD pattern to θ (Figure 5). For example, the intensity of the couplet becomes smaller when θ is close to 0° and 180°. These results indicated that the EDTM of azido vibrational modes may be approximated to lie on the line connecting N1 and N3. Azidomethane molecules and azidobenzene molecules each placed with θ of ca. –23° showed a negative-positive VCD couplet. The discrepancy between the VCD properties of these bimolecular computational systems and those of **5** suggested that the VCD signals generated from N=N=N stretching vibration is readily perturbed by molecular structures other than azido moieties. Thus, we recommend to always use theoretical calculations for interpreting azido VCD couplets.

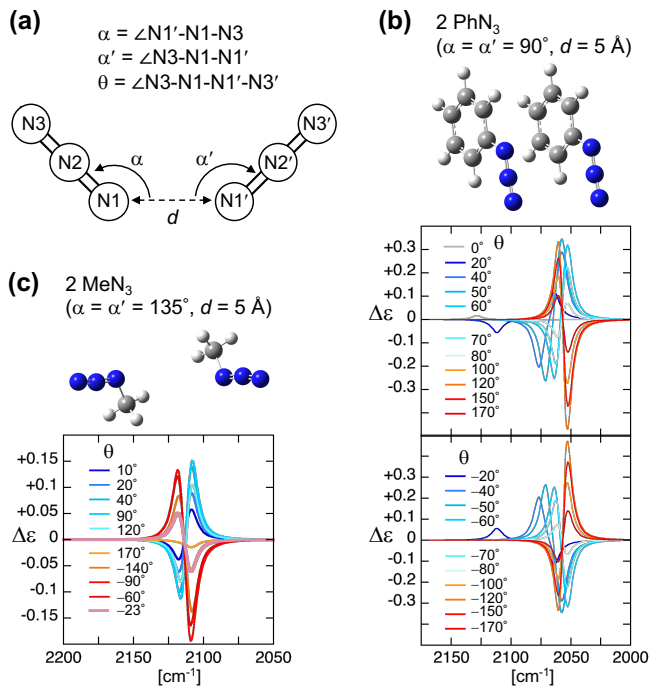

Fig. 5 Calculated VCD spectra of two simple azides as a function of the dihedral angle θ with fixed values of α, α′, and *d*. (a) Definitions of the values α, α′, *d*, and θ in this work. (b) Calculated VCD spectra of two azidobenzene molecules. Two phenyl groups are in *cis* orientation. (c) Calculated VCD spectra of two azidomethane molecules. Two methyl groups are in *trans* orientation. For both azidobenzene and azidomethane, structures with θ = 0° are drawn. Calculation conditions: B3PW91/6-311++G(d,p).

Conclusions

VCD spectroscopy is a useful technique to analyse the structure of biomolecules, but its use for biomacromolecules has been limited due to the low signal intensity and severe signal overlap. This study demonstrated that introduction of chromophores in

the 2300-2000 cm^{-1} region yields strong VCD signals that reflect molecular structures. Nitrile and isonitrile groups exhibited strong but complex anharmonic VCD signals. This work revealed that interplays between two chromophores enhance anharmonic VCD intensities. We also demonstrated a possibility that complex anharmonic VCD signals can be interpreted by means of anharmonic DFT calculations. Azido group is more advantageous due to its stronger VCD couplet whose pattern can be readily predicted by harmonic DFT calculations. In combination with other techniques (e.g., 2D IR, FRET and ESR), VCD spectroscopy using these chromophores should facilitate future structural studies of biomacromolecules in the solution state.

Conflicts of interest

There are no conflicts to declare.

Acknowledgements

This work was supported by KAKENHI Grant Nos. JP26702034, JP18H02093, JP18KK0394, and JP19H02836. M. Z. M. Z. is grateful for a scholarship from International Graduate Program (IGP), Hokkaido University. We thank Mr. Takahiro Kitahara for his initial synthetic effort.

Notes and references

1. N. Harada and K. Nakanishi, *J. Am. Chem. Soc.*, 1969, **91**, 3989-3991.
2. N. Harada and K. Nakanishi, *Circular dichroic spectroscopy : exciton coupling in organic stereochemistry*, University Science Books, 1983.
3. N. Harada, K. Nakanishi and N. Berova, in *Comprehensive Chiroptical Spectroscopy*, John Wiley & Sons, Inc., 2012, pp. 115-166.
4. N. Berova, L. D. Bari and G. Pescitelli, *Chem. Soc. Rev.*, 2007, **36**, 914-931.
5. N. Harada, *J. Am. Chem. Soc.*, 1973, **95**, 240-242.
6. T. F. Molinski, M. N. Salib, A. N. Pearce and B. R. Copp, *J. Nat. Prod.*, 2019, **82**, 1183-1189.
7. M. Satake, A. Morohashi, H. Oguri, T. Oishi, M. Hirama, N. Harada and T. Yasumoto, *J. Am. Chem. Soc.*, 1997, **119**, 11325-11326.
8. S. Abbate, F. Lebon, G. Longhi, S. E. Boiadjiev and D. A. Lightner, *J. Phys. Chem. B*, 2012, **116**, 5628-5636.
9. Y.-M. Shi, K. Hu, G. Pescitelli, M. Liu, X.-N. Li, X. Du, W.-L. Xiao, H.-D. Sun and P.-T. Puno, *Org. Lett.*, 2018, **20**, 1500-1504.
10. S. Matile, N. Berova, K. Nakanishi, S. Novkova, I. Philipova and B. Blagoev, *J. Am. Chem. Soc.*, 1995, **117**, 7021-7022.
11. K. Tsubaki, K. Takaishi, H. Tanaka, M. Miura and T. Kawabata, *Org. Lett.*, 2006, **8**, 2587-2590.
12. M. Balaz, J. D. Steinkruger, G. A. Ellestad and N. Berova, *Org. Lett.*, 2005, **7**, 5613-5616.
13. M. Balaz, A. E. Holmes, M. Benedetti, P. C. Rodriguez, N. Berova, K. Nakanishi and G. Proni, *J. Am. Chem. Soc.*, 2005, **127**, 4172-4173.
14. R. Wang, C. Geiger, L. Chen, B. Swanson and D. G. Whitten, *J. Am. Chem. Soc.*, 2000, **122**, 2399-2400.
15. J. Tabei, M. Shiotsuki, F. Sanda and T. Masuda, *Macromolecules*, 2005, **38**, 9448-9454.
16. G. Holzwarth and I. Chabay, *J. Chem. Phys.*, 1972, **57**, 1632-1635.
17. T. Taniguchi and K. Monde, *J. Am. Chem. Soc.*, 2012, **134**, 3695-3698.
18. T. Taniguchi, *Bull. Chem. Soc. Jpn.*, 2017, **90**, 1005-1016.
19. T. Hongen, T. Taniguchi, S. Nomura, J. Kadokawa and K. Monde, *Macromolecules*, 2014, **47**, 5313-5319.
20. K. Komori, T. Taniguchi, S. Mizutani, K. Monde, K. Kuramochi and K. Tsubaki, *Org. Lett.* 2014, **16**, 1386-1389.
21. G. Szilvagyi, B. Brem, G. Bati, L. Tolgyesi, M. Hollosi and E. Vass, *Dalton Trans.*, 2013, **42**, 13137-13144.
22. T. Asai, T. Taniguchi, T. Yamamoto, K. Monde and Y. Oshima, *Org. Lett.*, 2013, **15**, 4320-4323.
23. T. Asai, S. Morita, T. Taniguchi, K. Monde and Y. Oshima, *Org. Biomol. Chem.*, 2016, **14**, 646-651.
24. T. Taniguchi, D. Manai, M. Shibata, Y. Itabashi and K. Monde, *J. Am. Chem. Soc.*, 2015, **137**, 12191-12194.
25. C. I. Bautista-Hernández, R. E. Cordero-Rivera, E. A. Zúñiga-Estrada, N. Trejo-Carbajal, M. Meléndez-Rodríguez, O. R. Suárez-Castillo, M. Sánchez-Zavala, M. S. Morales-Ríos and P. Joseph-Nathan, *Tetrahedron Asymm.*, 2016, **27**, 623-638.
26. M. R. Poopari, Z. Dezhahang, K. Shen, L. Wang, T. L. Lowary and Y. Xu, *J. Org. Chem.*, 2015, **80**, 428-437.
27. Y. Hayashi, K. Nagai and S. Umemiya, *Eur. J. Org. Chem.*, 2019, **2019**, 678-681.
28. Y. Saito, M. Satake, R. Mori, M. Okayasu, H. Masu, M. Tominaga, K. Katagiri, K. Yamaguchi, S. Kikkawa, H. Hikawa and I. Azumaya, *Org. Biomol. Chem.*, 2020, **18**, 230-236.
29. K. Takaishi, K. Iwachido, R. Takehana, M. Uchiyama and T. Ema, *J. Am. Chem. Soc.*, 2019, **141**, 6185-6190.
30. T. Wu and X. You, *J. Phys. Chem. A*, 2012, **116**, 8959-8964.
31. C. L. Covington, V. P. Nicu and P. L. Polavarapu, *J. Phys. Chem. A*, 2015, **119**, 10589-10601.
32. V. P. Nicu, *Phys. Chem. Chem. Phys.*, 2016, **18**, 21202-21212.
33. S. Abbate, G. Mazzeo, S. Meneghini, G. Longhi, S. E. Boiadjiev and D. A. Lightner, *J. Phys. Chem. A*, 2015, **119**, 4261-4267.
34. S. Abbate, T. Bruhn, G. Pescitelli and G. Longhi, *J. Phys. Chem. A*, 2017, **121**, 394-400.
35. R. A. G. D. Silva, J. Kubelka, P. Bour, S. M. Decatur and T. A. Keiderling, *Proc. Nat. Acad. Sci.*, 2000, **97**, 8318-8323.
36. H.-Z. Tang, B. M. Novak, J. He and P. L. Polavarapu, *Angew. Chem. Int. Ed.*, 2005, **44**, 7298-7301.
37. R. Gangemi, G. Longhi, F. Lebon, S. Abbate and L. Laux, *Monatsh. Chem.*, 2005, **136**, 325-345.
38. L. Laux, V. Pultz, S. Abbate, H. A. Havel, J. Overend, A. Moscowitz and D. A. Lightner, *J. Am. Chem. Soc.*, 1982, **104**, 4276-4278.
39. A. T. Krummel and M. T. Zanni, *J. Phys. Chem. B*, 2008, **112**, 1336-1338.
40. K.-I. Oh, J.-H. Lee, C. Joo, H. Han and M. Cho, *J. Phys. Chem. B*, 2008, **112**, 10352-10357.
41. C. Fang, J. D. Bauman, K. Das, A. Remorino, E. Arnold and R. M. C. F. p. d. F. Hochstrasser, *Proc. Nat. Acad. Sci.*, 2008, **105**, 1472-1477.
42. U. Narayanan, T. A. Keiderling, C. J. Elsevier, P. Vermeer and W. Runge, *J. Am. Chem. Soc.*, 1988, **110**, 4133-4138.

43. U. Narayanan and T. A. Keiderling, *J. Am. Chem. Soc.*, 1988, **110**, 4139-4144.
44. T. Taniguchi, T. Suzuki, H. Satoh, Y. Shichibu, K. Konishi and K. Monde, *J. Am. Chem. Soc.*, 2018, **140**, 15577-15581.
45. M. J. Frisch, G. W. Trucks, H. B. Schlegel, G. E. Scuseria, M. A. Robb, J. R. Cheeseman, G. Scalmani, V. Barone, G. A. Petersson, H. Nakatsuji, X. Li, M. Caricato, A. V. Marenich, J. Bloino, B. G. Janesko, R. Gomperts, B. Mennucci, H. P. Hratchian, J. V. Ortiz, A. F. Izmaylov, J. L. Sonnenberg, D. Williams-Young, F. Ding, F. Lipparini, F. Egidi, J. Goings, B. Peng, A. Petrone, T. Henderson, D. Ranasinghe, V. G. Zakrzewski, J. Gao, N. Rega, G. Zheng, W. Liang, M. Hada, M. Ehara, K. Toyota, R. Fukuda, J. Hasegawa, M. Ishida, T. Nakajima, Y. Honda, O. Kitao, H. Nakai, T. Vreven, K. Throssell, J. A. Montgomery, Jr., J. E. Peralta, F. Ogliaro, M. J. Bearpark, J. J. Heyd, E. N. Brothers, K. N. Kudin, V. N. Staroverov, T. A. Keith, R. Kobayashi, J. Normand, K. Raghavachari, A. P. Rendell, J. C. Burant, S. S. Iyengar, J. Tomasi, M. Cossi, J. M. Millam, M. Klene, C. Adamo, R. Cammi, J. W. Ochterski, R. L. Martin, K. Morokuma, O. Farkas, J. B. Foresman, and D. J. Fox, *Gaussian 16*, *Rev A.03*, Wallingford CT, USA, 2016.
46. *Spartan 18*, Wavefunction Inc., Irvine, CA, USA, 2014.
47. G. Holzwarth, E. C. Hsu, H. S. Mosher, T. R. Faulkner and A. Moscowitz, *J. Am. Chem. Soc.*, 1974, **96**, 251-252.
48. P. L. Polavarapu, L. A. Nafie, S. A. Benner and T. H. Morton, *J. Am. Chem. Soc.*, 1981, **103**, 5349-5354.
49. P. Malon, L. J. Mickley, K. M. Sluis, C. N. Tam, T. A. Keiderling, S. Kamath, J. Uang and J. S. Chickos, *J. Phys. Chem.*, 1992, **96**, 10139-10149.
50. C. Shen, G. h. Loas, M. Srebro-Hooper, N. Vanthuyne, L. Toupet, O. Cador, F. Paul, J. T. López Navarrete, F. J. Ramírez, B. Nieto-Ortega, J. Casado, J. Autschbach, M. Vallet and J. Crassous, *Angew. Chem. Int. Ed.*, 2016, **55**, 8062-8066.
51. A. J. Schmitz, D. G. Hogle, X. S. Gai, E. E. Fenlon, S. H. Brewer and M. J. Tucker, *J. Phys. Chem. B*, 2016, **120**, 9387-9394.
52. Enantiomerically pure (+)-**2a** was reported in only one paper. While this reference depicted the structure of (*R*)-**2a**, it was labelled as (*S*)-enantiomer. We thus unambigously determined the absolute configuration of (+)-**2a** as *R* by using VCD spectroscopy as shown in Figure S3. J. Liu, H.-X. Zheng, C.-Z. Yao, B.-F. Sun and Y.-B. Kang, *J. Am. Chem. Soc.*, 2016, **138**, 3294-3297.
53. C. Merten, J. Bloino, V. Barone and Y. Xu, *J. Phys. Chem. Lett.*, 2013, **4**, 3424-3428.
54. M. Fusè, G. Mazzeo, G. Longhi, S. Abbate, M. Masi, A. Evidente, C. Puzzarini and V. Barone, *J. Phys. Chem. B*, 2019, **123**, 9230-9237.
55. C. Merten, *Phys. Chem. Chem. Phys.*, 2017, **19**, 18803-18812.
56. J. Y. Park, H.-J. Kwon, S. Mondal, H. Han, K. Kwak and M. Cho, *Phys. Chem. Chem. Phys.*, 2020, **22**, 19223-19229.
57. N. J. Agard, J. A. Prescher and C. R. Bertozzi, *J. Am. Chem. Soc.*, 2004, **126**, 15046-15047.

